10 Superconductivity and Magnetism

M. Bendele (since January 2009), D.G. Eshchenko (till January 2009), H. Keller, F. La Mattina (till June 2008), A. Maisuradze (till May 2008), P. Prem (since January 2009), J. Roos, S. Strässle, St. Weyeneth, B.M. Wojek, C. Duttwyler (Master student), U. Mosele (Master student, till August 2008)

Visiting scientists: M.V. Eremin, B. Graneli, V.A. Ivanshin, R. Puzniak, A. Shengelaya
Emeritus members: K.A. Müller (Honorarprofessor), T. Schneider (Titularprofessor), M. Mali

in collaboration with:
ETH Zürich (J. Karpinski), Paul Scherrer Institute (K. Conder, R. Khasanov, E. Morenzoni), Max-Planck-Institute for Solid State Research Stuttgart (A. Bussmann-Holder), IBM Rüschlikon Research Laboratory (J.G. Bednorz, S.F. Alvarado), University of Geneva (Ø. Fischer, J.M. Triscone), University of Rome (D. Di Castro), Kazan State University (A. Dooglav, M.V. Eremin, V. Ivanshin, B.I. Kochelaev), Polish Academy of Sciences (R. Puzniak), University of Belgrade (I.M. Savić), Tbilisi State University (A. Shengelaya), Iowa State University (A. Kaminski).

During the reporting period we continued our research activities in the field of novel electronic materials. We investigated their magnetic and electronic properties by combining experiments using microscopic tools, such as muon-spin rotation (μSR), electron paramagnetic resonance (EPR), nuclear magnetic resonance (NMR), nuclear quadrupole resonance (NQR), and the more macroscopic techniques of SQUID and torque magnetometry. From our various investigations we present in the following three studies which are currently of highest interest in this research field.

10.1 Oxygen isotope effects within the phase diagram of cuprates

In 1990 our group started a project on isotope effects in cuprate high-temperature superconductors (HTS's) which was initiated by K. Alex Müller. Several novel oxygen isotope (^{16}O/^{18}O) effects (OIE's) on different quantities in cuprates were observed by our group, such as on the transition temperature T_c (including site-selective OIE), the in-plane magnetic penetration depth $\lambda_{ab}(0)$ (including site-selective OIE), the anisotropy parameter γ, the pseudogap temperature T^*, the charge-ordering temperature T_{co}, the superconducting energy gap Δ_0, the Néel temperature T_N, the spin-glass freezing temperature T_g, and the EPR line width Γ (1; 2; 3; 4). These unconventional OIE's were detected in different cuprate HTS families by using various types of samples (powders, single crystals, films) and experimental techniques (SQUID, magnetic torque, μSR, EPR, XANES, neutron scattering).

Cuprate HTS's exhibit a rich phase diagram (Fig. 10.1). The undoped parent compounds are characterized by a long range 3D antiferromagnetic (AFM) order, which is rapidly destroyed when holes are doped into the CuO_2 planes. Short-range AFM correlations survive, however, well in the superconducting (SC) region of the phase diagram by forming a spin-glass (SG) state. Upon the onset of superconductivity this phase persists for a limited doping range, suggesting that SC and SG phases coexist within a certain doping range. With increasing doping, the superconducting transition temperature T_c increases. Correspondingly, four phases can be differentiated: the AFM phase, the SG phase, the SG+SC phase, and the SC phase. How these phases are re-

lated to each other is an open and controversial issue, and until now experiments are missing which could provide a fundamental link between them. In particular, it is very interesting to investigate the OIE's on the corresponding transition temperatures between the various phases.

Years ago we observed a huge OIE on the spin-glass freezing temperature T_g in $La_{2-x}Sr_xCu_{1-z}Mn_zO_4$ ($x = 0.03$ and 0.05; $z = 0.02$) by means of μSR (5). This is a clear signature that the spin dynamics in cuprates are ultimately correlated with lattice vibrations.

Recently, we performed a detailed OIE study of the various phases (SC, SG+SC, SG, AFM) in the prototype cuprate system $Y_{1-x}Pr_xBa_2Cu_3O_{7-\delta}$ by means of μSR and magnetization experiments (6). These techniques have the advantage of being direct, bulk sensitive, unambiguous, and able to measure T_c as well as T_g in the region where both coexist. The results are sumarized in Figs. 10.1 and 10.2 (6).

All phases exhibit an OIE which is strongest, where the respective phase terminates. Note that the OIE on the magnetic phases (SG and AFM) are sign reversed as compared to the one on the superconducting phase. Another interesting anti-correlation is observed in the region where spin-glass magnetism coexists with superconductivity (SG+SC). Here a small OIE on T_c corresponds to a large OIE on T_g in sequence and vice versa. This behavior suggests that in this regime phase separation sets in where the superfluid density coexists with a SG related one. Since the isotope effect on T_c can be accounted for through polaron formation (7), the one on T_g is expected to originate from the same physics. By relating the AFM transition temperature to the metal-insulator transition, a reduction in kinetic energy caused by polaron formation is proposed to explain this OIE as well. The various OIE's reported here, clearly evidence that lattice effects are effective in all phases of cuprate superconductors and impose serious constraints on theories for cuprate superconductivity.

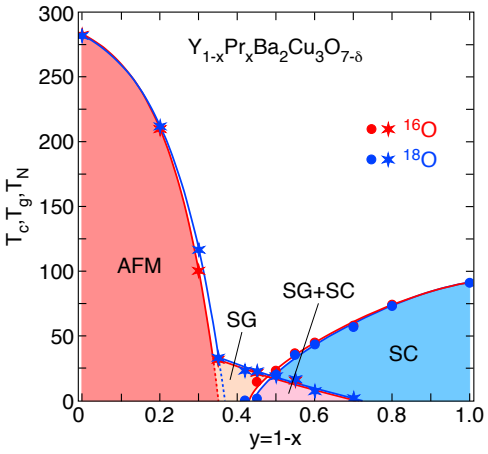

Figure 10.1: Dependence of the superconducting transition (T_c), the spin-glass ordering (T_g), and the antiferromagnetic ordering (T_N) temperatures for $^{16}O/^{18}O$ substituted $Y_xPr_{1-x}Ba_2Cu_3O_{7-\delta}$ on the Pr content x. The solid lines are guides to the eye. The areas denoted by "AFM", "SG", and "SC" represent the antiferromagnetic, the spin-glass, and the superconducting regions, respectively. "SG+SC" corresponds to the region where spin-glass magnetism coexists with superconductivity. After [6].

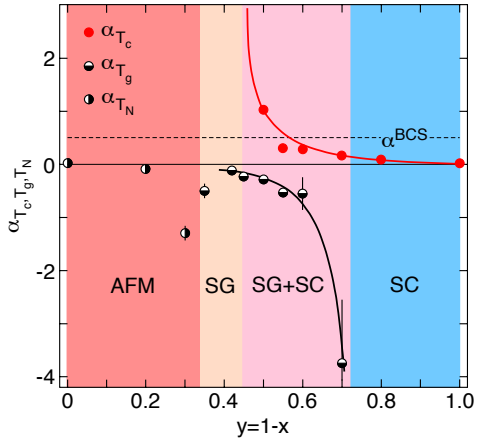

Figure 10.2:
OIE exponents α_{T_c}, α_{T_g}, and α_{T_N} for $^{16}O/^{18}O$ substituted $Y_xPr_{1-x}Ba_2Cu_3O_{7-\delta}$ as a function of the Pr content x. The dashed line corresponds to $\alpha_{T_c}^{BCS}$=0.5. The solid lines are guides to the eye. The meaning of the areas denoted by "AFM", "SG", "SG+SC", and "SC" are the same as in Fig. 10.1. After [6].

[1] D. Zech, H. Keller, K. Conder, E. Kaldis, E. Liarokapis, N. Poulakis, and K.A. Müller, Nature (London) **371**, 681 (1994).

[2] G.-M. Zhao, M.B. Hunt, H. Keller, and K.A. Müller, Nature (London) **385**, 236 (1997).

[3] G.-M. Zhao, H. Keller, and K. Conder J. Physics: Condens. Matter **13**, R569 (2001).

[4] H. Keller, in *Superconductivity in Complex Systems*, Structure and Bonding Vol. **114**, eds. A. Bussmann-Holder and K.A. Müller (Springer-Verlag Berlin Heidelberg 2005), pp. 143-169.

[5] A. Shengelaya, G.-M. Zhao, C. Aegerter, K. Conder, I.M. Savić, and H. Keller, Phys. Rev. Lett. **83**, 5142 (1999).

[6] R. Khasanov, A. Shengelaya, D. Di Castro, E. Morenzoni, A. Maisuradze, I.M. Savić, K. Conder, E. Pomjakushina. A. Bussmman-Holder, and H. Keller, Phys. Rev. Lett. **101**, 077001 (2008).

[7] A. Bussmann-Holder and H. Keller, in Polarons in Advanced Materials, ed. A.S. Alexandrov (Springer Series in Materials Science 103, Canopus Publishing, Bristol 2007), pp. 599-621.

10.2 Temperature dependent anisotropy parameter in the novel iron-pnictide superconductors

Since the discovery of high-temperature superconductivity in the cuprate superconductors, much effort has been spent on finding similar superconducting transition-metal based oxides. The discovery of superconductivity at $T_{\rm c} \simeq 26$ K for $LaFeAsO_{1-x}F_x$ (La1111) in 2008 by Hosono and coworkers triggered great interest in the scientific community (1). Soon after, by substituting La with other lanthanide ions like Ce, Pr, Nd, Sm, Gd, Tb, and Dy, a series of novel superconducting materials was synthesized with T_c's up to 56 K (2).

All these iron-pnictide superconductors have a layered crystal structure containing Fe_2As_2-sheets, where the Fe ions are arranged on simple square lattices (1). Superconductivity takes place in the Fe_2As_2-layers, whereas the spacing layers are charge reservoirs when doped with holes or electrons. These novel iron-based superconductors are in many respects similar to the cuprates, and it is interesting to compare their physical properties. However, in order to investigate the anisotropic properties of these superconductors, single crystals of high quality are required. In the last year we performed a detailed study of the anisotropy parameter in single crystals of the Ln1111 (Ln= Lanthanide) family by means of torque magnetometry (3; 4).

High quality single crystals of the Ln1111 family were grown using the cubic anvil high-pressure technique at ETH Zurich (5). The rectangular plate-like crystals have typical masses of 0.1 - 6 μg. The crystal structure was checked by means of X-ray diffraction revealing the c axis to be perpendicular to the plates. Selected crystals were characterized in a SQUID magnetometer.

In order to investigate the anisotropic properties of the Ln1111 family, we studied the angular dependence of the superconducting torque in a tilted magnetic field with respect to the crystallographic axes. The torque was found to be best described by using a two-anisotropy model (6), where the anisotropy of the magnetic penetration depth $\gamma_\lambda = \lambda_c/\lambda_{ab}$ and the anisotropy of the upper critical field $\gamma_H = H_{\rm c2}^{ab}/H_{\rm c2}^{c}$ enter distinctly into the theoretical description of the data. Here λ_i and $H_{\rm c2}^{i}$ denote the magnetic penetration depth and the upper critical field of the material, respectively, with the magnetic field oriented along the crystallographic i axis. Some examples of angular dependent torque data are depicted in Fig. 10.3.

The final result of this anisotropy study for three different crystals of the compounds $SmFeAsO_{0.8}F_{0.2}$ and $NdFeAsO_{0.8}F_{0.2}$ with $T_{\rm c}$'s

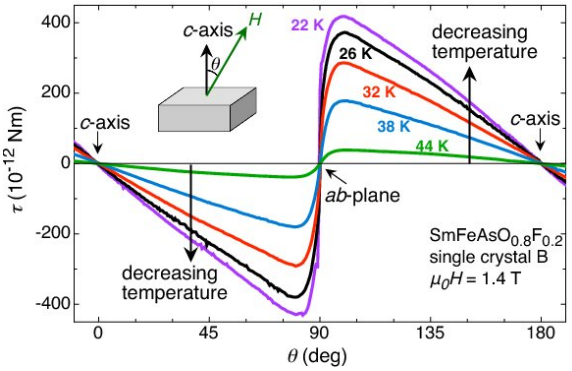

Figure 10.3: Angular dependence of the reversible torque data for $SmFeAsO_{0.8}F_{0.2}$ at several temperatures derived in a magnetic field of 1.4 T. For clarity not all measured data are shown.

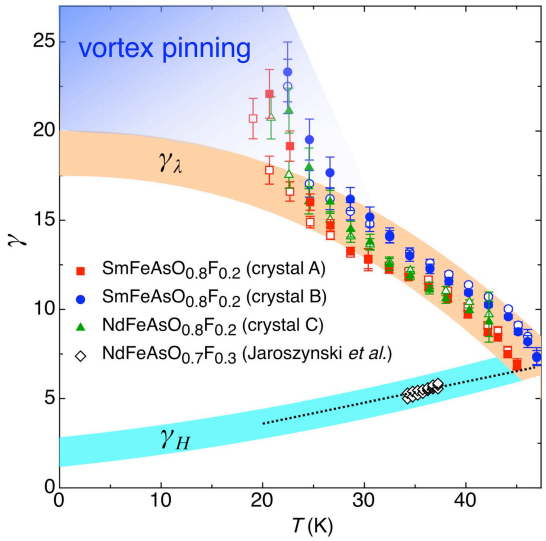

Figure 10.4: Summary of the systematic analysis of the torque data of single crystals $SmFeAsO_{0.8}F_{0.2}$ (crystal A and B) and $NdFeAsO_{0.8}F_{0.2}$ (crystal C). Values of γ (open symbols) and γ_λ (closed symbols) were obtained from fits to the data. The upper broad orange band is a guide to the eye, suggesting an estimate of $\gamma_\lambda(0) \approx 19$. The dotted line is the linear extrapolation of γ_H obtained from resistivity measurements [7] on a $NdFeAsO_{0.7}F_{0.3}$ single crystal with similar $T_c \simeq 45$ K (diamonds). The lower broad blue band is a guide to the eye, suggesting an estimate of $\gamma_H(0) \approx 2$. At low temperatures, the fitted anisotropy exceeds the guide to the eye, since substantial pinning contributions to the torque influence the determination of the anisotropy parameter.

in the range of 45 K is summarized in Fig. 10.4. We found strong evidence that the two anisotropies γ_λ and γ_H are different and depend strongly on temperature (3; 4). This implies that superconductivity in the oxypnictides is unconventional, since for conventional Ginzburg-Landau superconductors, the anisotropy parameter is a unique quantity, independent on temperature and field. Torque magnetometry in low magnetic fields is very sensitive to γ_λ which exhibits a pronounced increase with decreasing temperature. This is in contrast to the behavior of γ_H which according to recent resistivity measurements decreases with decreasing temperature (7). Close to T_c both anisotropies have very similar values of $\gamma_\lambda(T_c) \approx \gamma_H(T_c) \approx 7$, whereas at low temperatures the magnetic penetration depth anisotropy $\gamma_\lambda(0) \approx 19$ and the upper critical field anisotropy $\gamma_H(0) \approx 2$. This behavior is similar to that in the two-band superconductor MgB_2 (although $\gamma_\lambda(T)$ and $\gamma_H(T)$ have reversed slopes) where the temperature dependences of $\gamma_\lambda(T)$ and $\gamma_H(T)$ are well understood (8). This result strongly suggests multiband superconductivity in the novel class of oxypnictide superconductors.

[1] Y. Kamihara, T. Watanabe, M. Hirano, and H. Hosono, J. Am. Chem. Soc. **130**, 3296 (2008).

[2] Z. Bukowski, S. Weyeneth, R. Puzniak, P. Moll, S. Katrych, N.D. Zhigadlo, J. Karpinski, H. Keller, and B. Batlogg, Phys. Rev. B **79**, 104521 (2009).

[3] S. Weyeneth, R. Puzniak, U. Mosele, N.D. Zhigadlo, S. Katrych, Z. Bukowski, J. Karpinski, S. Kohout, J. Roos, and H. Keller, J. Supercond. Nov. Magn. **22**, 325 (2009).

[4] S. Weyeneth, R. Puzniak, N.D. Zhigadlo, S. Katrych, Z. Bukowski, J. Karpinski, and H. Keller, J. Supercond. Nov. Magn. **22**, 347 (2009).

[5] N.D. Zhigadlo, S. Katrych, Z. Bukowski, S. Weyeneth, R. Puzniak, and J. Karpinski, J. Phys.: Condens. Matter **20**, 342202 (2008).

[6] V.G. Kogan, Phys. Rev. B **24**, 1572 (1981) and V.G. Kogan, Phys. Rev. Lett. **89**, 237005 (2002).

[7] J. Jaroszynski, F. Hunte, L. Balicas, Y.-J. Jo, I. Raicevic, A. Gurevich, D.C. Larbalestier, F.F. Balakirev, L. Fang, P. Cheng, Y. Jia, and H.-H. Wen, Phys. Rev. B **78**, 174523 (2008).

[8] M. Angst, R. Puzniak, A. Wisniewski, J. Jun, S.M. Kazakov, J. Karpinski, J. Roos, and H. Keller, Phys. Rev. Lett. **88**, 167004 (2002).

10.3 NMR investigations of orbital current effects in YBCO compounds

The possible existence and role of a hidden order parameter in the phase diagram of high-T_c superconductors are highly debated issues not only in cuprates but in high-T_c physics in general. Among the concepts of broken symmetry, the d-density wave (DDW) order (1) and the circulating-current (CC) picture (2) are the most prominent proposals. The characteristic of these models are currents, which are believed to flow in the CuO_2 planes of cuprate superconductors.

Besides photoemission evidence for dichroism (3), reports on polarized neutron scattering data claim consistency with such an ordered phase (*e.g.* (4; 5)). However, the experimental situation remains controversial and it is highly desirable to use a more local probe, like nuclear magnetic resonance (NMR), to search for such orbital currents (OC's). For NMR, the relevant feature of OC formation is the resulting internal magnetic field distribution. For symmetry reasons, additional OC fields at the Y site in YBCO compounds point either along or perpendicular to the crystalline c axis for any of the proposed current patterns. Such current patterns are expected to form when the material enters the so-called pseudogap phase. With this phase a peculiar partial gap at the Fermi surface is associated, which still lacks a satisfying microscopic description. It is generally agreed, that a detailed understanding of the pseudogap phase is essential to solve the mystery of high-temperature superconductivity.

We completed our ^{89}Y NMR investigation of oriented powder samples of $Y_2Ba_4Cu_7O_{15-\delta}$ (Y247) to search for OC effects. Y247 exhibits a doping difference of Y neighboring CuO_2 planes which prevents a possible complete cancellation of fields due to OC circulating in adjacent planes. We found no clear evidence for the appearance of an OC phase in this specific compound (6). Nevertheless, we provide limits for static magnetic fields and fluctuating field amplitudes, which constitute meaningful constraints to theoretical models.

Typical NMR spectra are displayed in Figs. 10.5 a, b. In the Y247 compound the Knight shift drops significantly as one lowers the temperature below $200\,\mathrm{K}$, which is evidence for the opening of a pseudogap (Fig. 10.5 c).

To check for static magnetic fields, showing up at the Y site when entering the pseudogap phase, the temperature dependence of the leading-edge line width of the NMR absorption line was determined (Fig. 10.5 d). Additional static magnetic fields influence the NMR line only when pointing along the externally applied field. Conservatively, the total observed broadening in the investigated temperature range was taken to deduce an upper limit for a static OC effect, although both field orientations show the same broadening within measurement uncertainties. From our experiments we find a limit of $0.15\,\mathrm{mT}$ for an additionally in the pseudogap phase appearing static magnetic field at the Y site in Y247.

For the spin-lattice relaxation process only fields fluctuating perpendicular to the quantization axis are relevant. Hence, the occurrence of fluctuating OC must alter the ratio between the spin-lattice relaxation rate measured for the external field directed along $(1/T_1^{\parallel})$ and perpendicularly $(1/T_1^{\perp})$ to the c axis. The temperature dependence of the spin-lattice relaxation rate ratio was mea-

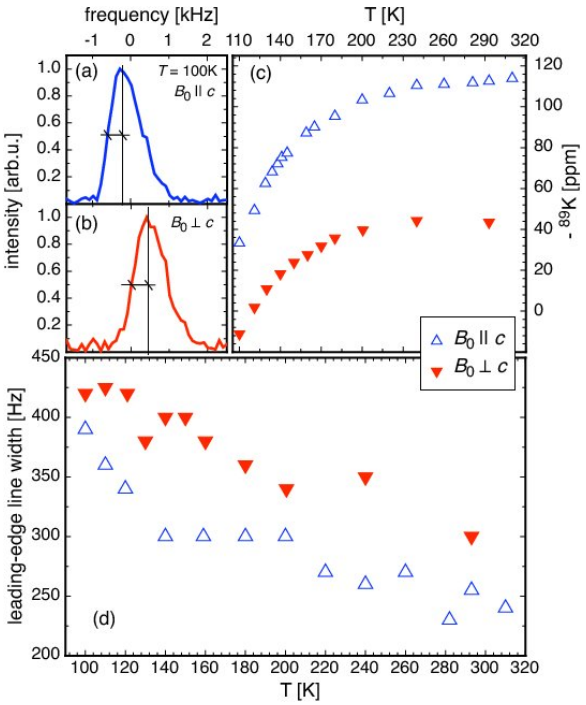

Figure 10.5: ^{89}Y NMR data of c-axis aligned powder measured in a $9\,\mathrm{T}$ field orientated parallel (‖) or perpendicular (⊥) to c. (a),(b): typical absorption lines at $100\,\mathrm{K}$ for both field orientations; (c): temperature dependent magnetic shift; (d): temperature dependent leading-edge line width at half height.

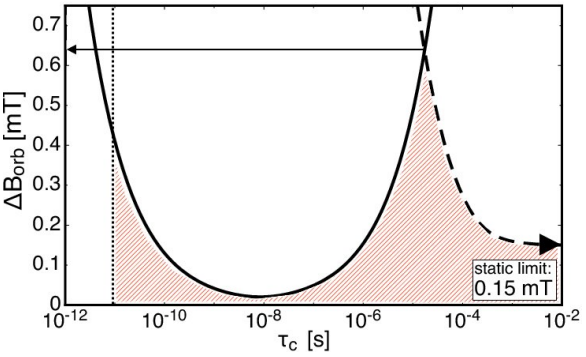

Figure 10.6: Dependence of the possible OC field amplitude ΔB_{orb} on the OC correlation time τ_c from ^{89}Y nuclear spin-lattice relaxation measurements in Y247 at $100\,\mathrm{K}$ (solid line, see text). Lower limit of τ_c from neutron (dotted) and upper limit of τ_c from line width measurements (dashed line) are shown. The maximum static field $\lesssim 0.15\,\mathrm{mT}$ is included. The shaded area represents all ΔB_{orb} consistent with measurements.

sured in the normal conducting state up to room temperature, covering the pseudogap regime. Within measurement error no change of this ratio was observed. Using a simple relaxation model the maximum field amplitude ΔB_{orb} consistent with measurement uncertainties was determined in dependence of the correlation time τ_c of fluctuating OC fields (6) (solid line in Fig. 10.6).

To limit τ_c towards the slow fluctuation regime, we included in our line-width analysis motional narrowing behavior (dashed line in Fig. 10.6). For the cutoff in the fast fluctuation regime we used results of reports on neutron scattering (4), where it was stated that the anomalous magnetism observed and related to OC is static on the neutron time scale. From Fig. 10.6 it is evident that a fluctuating magnetic field, which may appear at the Y site in the pseudogap phase of Y247 cannot exceed $0.7\,\mathrm{mT}$.

[1] S. Chakravarty, R.B. Laughlin, D. K. Morr, and Ch. Nayak, Phys. Rev. B **63**, 094503 (2001).

[2] C.M. Varma, Phys. Rev. B **73**, 155113 (2006).

[3] A. Kaminski, S. Rosenkranz, H.M. Fretwell, J.C. Campuzano, Z. Li, H. Raffy, W.G. Cullen, H. You, C.G. Olson, C.M. Varma, and H. Höchst, Nature **416**, 610 (2002).

[4] B. Fauque, Y. Sidis, V. Hinkov, S. Pailhes, C.T. Lin, X. Chaud, and P. Bourges, Phys. Rev. Lett. **96**, 197001 (2006).

[5] Y. Li, V. Baledent, N. Barisic, Y. Cho, B. Fauque, Y. Sidis, G. Yu, X. Zhao, P. Bourges, and M. Greven, Nature **455**, 372 (2008).

[6] S. Strässle, J. Roos, M. Mali, and H. Keller, Phys. Rev. Lett. **101**, 237001 (2008).